

the $E_{\text{He}}^{\text{ad}}$ depends largely on the shape of the interstitial site. The average value of the helium adsorption energy differs for different type of interstitial site, and the CTP sites hold the lowest average adsorption energy for helium in tungsten. Moreover, the $E_{\text{He}}^{\text{ad}}$ varies prominently even for the same type of interstitial site. To understand the large variation of the helium adsorption energies, volumes V of the interstitial sites at clean GBs without helium are measured and are plotted at the bottom of Fig. 1 (a). There is an obvious correlation between the helium adsorption energies and the volumes of the interstitial sites. That is, the larger the volume is, the lower the helium adsorption energy is. The $E_{\text{He}}^{\text{ad}}$ versus V is plotted in Fig. 1 (b). To validate our final conclusion, the helium adsorption energies in vacancies around GBs are also plotted in Fig. 1 (b). It is obviously that the $E_{\text{He}}^{\text{ad}}$ exponentially decreases as the volumes of interstitial sites increase. Helium is expected to occupy the interstitial sites with larger volume, since helium has a closed shell electronic structure and the bonding interaction is weak^[3].

References

- [1] C. S. Becquart, C. Domain, Nucl. Instr. and Meth. B, 255(2007)23.
- [2] M. F. Ashby, F. Spaepen, S. Williams, Acta Metall., 26(1978)1647.
- [3] X. T. Zu, L. Yang, F. Gao, et al., Phys. Rev. B, 80(2009)054104.

4 - 14 First-principles Investigation of Helium Segregations at Grain Boundaries in Tungsten

He Wenhao, Gao Xing and Wang Zhiguang

Tungsten is one of the promising candidates for plasma facing materials (PFMs), such as the first wall materials and divertor, of the magnetic confinement fusion reactor due to its high melting temperature, high thermal conductivity and low sputtering erosion. The PFMs will be exposed to a high flux of helium atoms escaping from the plasma^[1]. The helium atoms in metals tend to assemble in vacancies, dislocations, and grain boundaries (GBs), and form helium bubbles, which can significantly degrade the mechanical properties of materials. One well-known example is the high-temperature helium embrittlement (HE). It has been experimentally demonstrated that the segregation of helium at GBs is sensitive to the morphology of GBs^[2]. Therefore it is possible to enhance HE resistance of materials by increasing the fraction of certain kinds of GBs which are resistant to aggregation of helium atoms through GB engineering. To provide a rational guidance for the GB engineering, it is of fundamental importance to explore the relationship between the segregations of helium atoms at GBs and the characteristics of GBs.

First-principles calculations of total energy were carried out with the Vienna Ab initio Simulation Package (VASP) based on the density functional theory (DFT). The projected augmented wave (PAW) pseudopotentials were employed in the calculations within the generalized gradient approximation (GGA) with Perdew and Wang functional for the exchange and correlation energies. A cutoff energy of 400 eV was used for the plane-wave expansion. The internal structure relaxations stopped when the residual force on each atom was less than 0.01 eV/Å. By least-square-fitting total energies to the 4th Murnaghan's equation of state, the calculated equilibrium lattice parameter of the body centered cubic tungsten was 3.19 Å. To investigate the segregation behavior of helium at GBs, eight low sigma number symmetric tilt GBs with [001], [110], and [111] as tilt axes were constructed with the CSL model. The interstitial sites at grain boundaries are identified with five types of deltahedra, that is, tetrahedron (TET), octahedron (OCT), pentagonal bipyramid (PBP), cap trigonal prism (CTP), and bitetrahedron (BTE)^[3].

The helium segregation energy $E_{\text{He}}^{\text{seg},i}$ in the i^{th} type interstitial site at GBs can be calculated by

$$E_{\text{He}}^{\text{seg},i} = (E_{\text{GB}}^{\text{He},i} - E_{\text{GB}}^{\text{Perf}}) - (E_{\text{bulk}}^{\text{He}} - E_{\text{bulk}}^{\text{Perf}}), \quad (1)$$

where $E_{\text{GB}}^{\text{He},i}$ is the total energy of the supercell with a helium atom in the i^{th} type of interstitial site at a GB, $E_{\text{GB}}^{\text{Perf}}$ is the total energy of the supercell containing clean GB, and $E_{\text{bulk}}^{\text{He}}$ is the total energy of the supercell with a helium atom in the TET interstitial site in bulk, $E_{\text{bulk}}^{\text{Perf}}$ is the total energy of the bulk without helium. For a GB, the helium prefers to segregate to the interstitial sites with the lowest segregation energy, which is defined as the helium segregation energy in the GB $E_{\text{He}}^{\text{seg,GB}}$. The $E_{\text{He}}^{\text{seg,GB}}$ in the eight GBs are listed in Table 1.

Table 1 The helium segregation energy $E_{\text{He}}^{\text{seg,GB}}$ in the eight GBs.

	$E_{\text{He}}^{\text{seg,GB}}/\text{eV}$	GBs	$E_{\text{He}}^{\text{seg,GB}}/\text{eV}$	GBs	$E_{\text{He}}^{\text{seg,GB}}/\text{eV}$
$\sum 3(110)[111]$	-1.23	$\sum 5(310)[001]$	-2.65	$\sum 3(111)[110]$	-3.44
$\sum 5(210)[001]$	-2.21	$\sum 11(332)[110]$	-2.84	$\sum 19(116)[110]$	-3.74
$\sum 9(114)[110]$	-2.60	$\sum 17(410)[001]$	-3.31		

Clearly, the helium segregation energy in GB $\Sigma 3(110)[111]$ is the largest among the eight GBs studied here, which means that GB $\Sigma 3(110)[111]$ is unfavorable to the segregation of helium atoms compared to other GBs studied here. Unfortunately, we did not find any experimental study about the effect of various types of GBs on the segregation of helium atoms in tungsten so far.

References

- [1] S. J. Zinkle, Phys. Plasmas, 12(2005)058101.
- [2] N. Sakaguchi, Y. Ohguchi, T. Shibayama, et al., J. Nucl. Mater., 432(2013)23.
- [3] M. F. Ashby, F. Spaepen, S. Williams, Acta Metall., 26(1978)1647.

4 - 15 Progress of Materials Research in 2016

Liu Jie

In the year 2016, the materials research at the Institute of Modern Physics (IMP), Chinese Academy of Sciences has gained significant progress, including simulation of single event effects, nano research, irradiation effects of solid materials. These achievements represent that the materials research at IMP has reached a new level, benefiting from the accumulation of the past few years.

Simulation of single event effects

Large scale integrated circuits working in space interact with various particles and the interactions give rise to a variety of physical phenomena, known as single event effects (SEEs). SEEs can threaten the safety of spacecrafts and, sometimes, induce serious disasters. To reduce the risks, accelerators-based ground simulation of SEEs of electronic devices represents a crucial strategy before launching a spacecraft. The accelerator Cooling Storage Ring (CSR) of Heavy Ion Research Facility in Lanzhou (HIRFL), a world-level large scale accelerator, can accelerate ions with energies up to hundreds GeV/u, providing an ideal irradiation source for SEEs research. To promote this application, an advanced evaluation platform connected to CSR is highly desired. Constructing such a platform has been approved by National Science and Technology Major Project. The approval represents a milestone event for the SEEs research of China.

Nano Research

Ion-track technology is a unique method for creating novel nanostructures. In the past year, a unique copper nanostructure with conical shape, vertical alignment, large ratio of cone height and curvature radius at the apex, controlled cone angle, and single-crystal structure has been successfully fabricated by the ion track technology, which is considered an ideal candidate for enhancing field electron-emission efficiency with additional merits such as good mechanical and thermal stability, see Fig. 1. Such copper nanostructure shows super-sharp tip and a

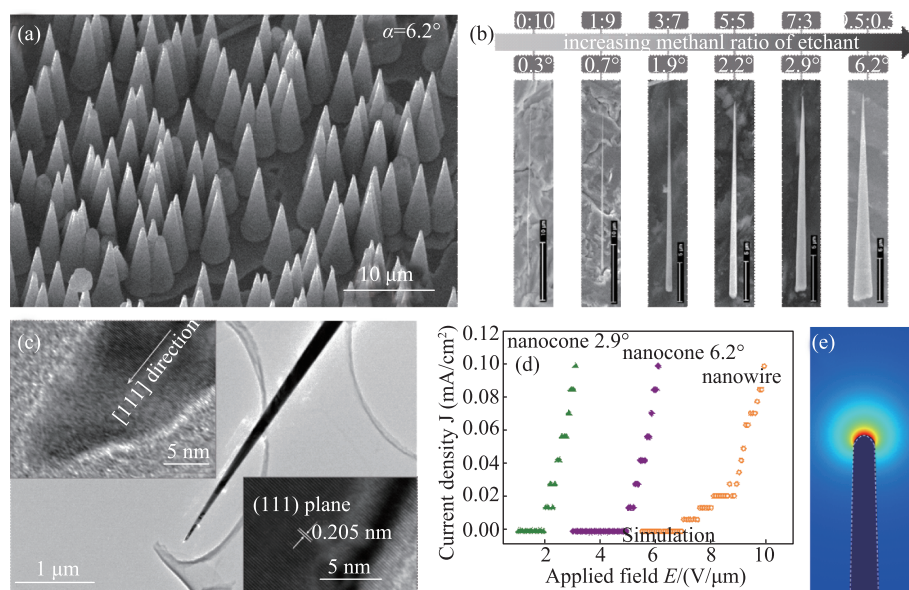


Fig. 1 (color online) Morphology and electron field emission of arrays of super-sharp nanocone. (a) Scanning electron microscopic (SEM) image of a nanocone array, (b) SEM of image of tunable nanocones with tunable cone angle, (c) Transmission electron microscopic image of a super-sharp nanocone with curvature radius of 3 nm, (d) Field emission of nanocone arrays with different cone angles and an array of nanowire, (e) Finite element analysis of local field distribution.